

# Cloud Free Flood Mapping: Towards a Radar-Based Approach to Flood Detection for Index Insurance Applications in Northern Bangladesh

M. Thomas<sup>1</sup>, E. Tellman<sup>2</sup>, P. Colosio<sup>3</sup>, M. Tedesco<sup>4</sup>, M.S. Steckler<sup>4</sup>

<sup>1</sup>*Columbia University*, <sup>2</sup>*Earth Institute, Columbia University*, <sup>3</sup>*University of Brescia*, <sup>4</sup>*Lamont Doherty Earth Observatory, Columbia University*

## Abstract:

New types of financial instruments, such as index insurance, are being piloted in flood-prone Bangladesh. Current remote-sensing flood index insurance contracts in Bangladesh rely on optical satellite sensors (MODIS) for flood detection. Radar-based satellites can penetrate clouds, offering more consistent mapping during flood events. Here we investigate the feasibility of radar sensors to estimate inundation in Northern Bangladesh by analyzing performance from Sentinel-1 Synthetic Aperture Radar (SAR) (every 6–12 days at 10m resolution since 2014) and SSM/I Passive Microwave sensors (twice daily at 3.125 km resolution since 1992). A Synthetic Aperture Radar time series is developed from Sentinel-1 in Google Earth Engine by using a time series approach to identify statistically anomalous drops in backscatter for each pixel. We adapt the DeVries et al. (2020) Sentinel-1 flood detection algorithm to i) estimate inundated area with each satellite overpass, ii) employ post processing to improve accuracy, iii) adjust image baselines to account for local irrigation dynamics in Northern Bangladesh. We use the SSM/I time series to estimate flooded area from changes in brightness temperature by implementing the De Groot and Riva (2009) algorithm. We compare each flooded area time series to river water level data in Northern Bangladesh to assess consistency in the signal and select specific flood events to assess accuracy of flood area predictions. Comparisons to river water level data reveal Sentinel-1 provides a more consistent flood signal than the noisier signal of SSM/I. Comparison of radar flood maps to optical data (Sentinel-2) of an April 2017 flood over a 7.4 km<sup>2</sup> region in Sylhet finds higher flooded area accuracy from Sentinel-1 ( $F_1 = 0.92$ , 74,000 pixels) than from SSM/I ( $F_1 = 0.63$ , <1 pixel). Preliminary results indicate Sentinel-1 can support an inundation time series suitable for index insurance triggers despite observation frequency limitations, while an SSM/I time series could provide valuable long-term risk assessment for insurance purposes. However, more work is needed to improve the accuracy of an SSM/I time series for index insurance applications.

## I. Introduction

Despite Bangladesh being one of the most flood-prone countries in the world, farmers currently have little economic security to protect against flood damage. While monsoon-season flooding is a typical and often an important reality for farmers, an off-season or particularly severe flood can mean losing an entire season of crops.

In recent years, different financial instruments have been piloted in the region to take economic burden off of farmers. One such device, flood index insurance, employs a data driven index to deliver payouts upon that index exceeding a predetermined threshold. Satellite remote sensing technology is often implemented to serve as a primary or secondary source of flood extent data which can inform the degree to which a certain region receives

an insurance payout. However current implementations in the region use optical satellites (MODIS) which cannot gather data under clouds and can only deliver readings at a moderate spatial resolution of 250 m (Amarnath, 2020).

Radar based satellite technologies provide a compelling alternative to optical sensors due to their ability to pass through the cloud cover which often obscures flood images and their wide range of available resolutions and observation frequencies. High resolution radar satellites, such as the European Space Agency's Sentinel-1 Synthetic Aperture Radar (SAR) constellation, have demonstrated the possibility of high-resolution

cloud-free flood mapping (Landuyt et al., 2019). Meanwhile Passive Microwave sensors such as NASA's Special Sensor Microwave / Imager (SSM/I) offer the possibility of a daily flood extent time series from 1979-Present (DeGrove and Riva, 2009), which could provide valuable temporal specificity risk assessment necessary for a radar flood index insurance implementation.

Here we explore the development of an inundation time series from both Sentinel-1 and SSMI and analyze each time series' ability to serve as an accurate inundation indicator for flood index insurance. We aim to analyze each sensor for consistency and accuracy with considerations to observation frequency, resolution, and historical availability.

## II. Background and study site



Figure 1: Map of Northern Bangladesh showing districts on the Brahmaputra (left) and the Haor basin (right). Districts studied, Jamalpur and Sylhet, are shaded in grey.

Northern Bangladesh sees regular flood events as part of a typical monsoon season (approx. June-September).

Along the Brahmaputra river in districts such as Jamalpur, this often takes the form of river overflow from the Brahmaputra. From preliminary qualitative optical data observations, this flooding is often uneven and fragmented into many small rivers, canals, and lakes, as seen in Figure 1. Flooding in this region occurs annually in the summertime

monsoon season, however especially severe flood years can nevertheless cause significant damage.

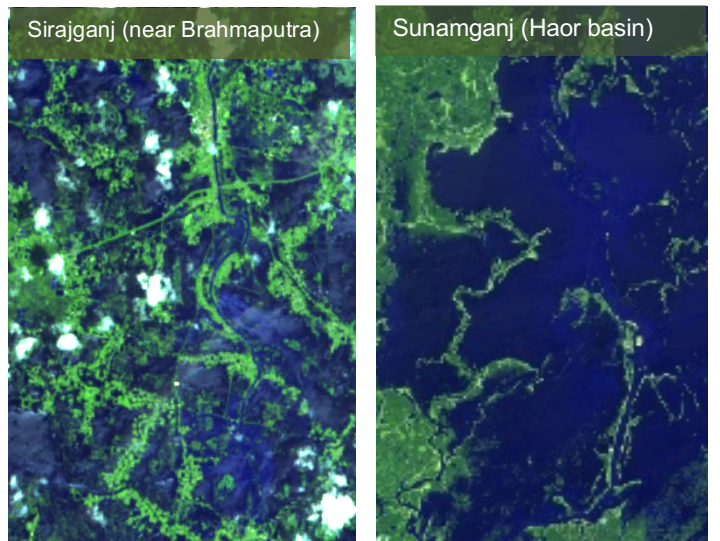


Figure 2: Left: Monsoon season flooding in Sirajganj District, 2017 (adjacent to Brahmaputra river). Right: April 2017 flooding in Sunamganj District (Haor Region). Images from Sentinel-2 with RGB = (SWIR2, SWIR1, Red).

% Area in Bangladesh Flooded, 2014-2019

Source: Bangladesh Flood Forecasting and Warning Center (FFWC)

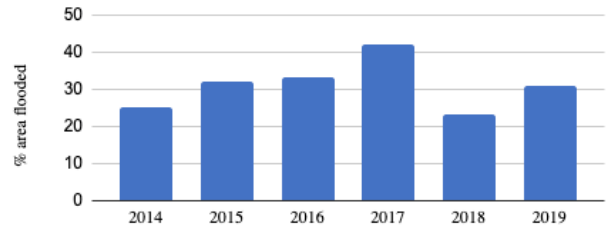


Figure 3: Flood extent data from Bangladesh Government records

Because 2017 represents the most severe flood year 2014-2019 (Fig. 3) and significant Sentinel-1 data is available starting then (Fig. 4), the entire year of 2017 over the Jamalpur District was chosen for water level comparisons to assess algorithm accuracy in the geography of Brahmaputra regions. Furthermore, we examine the July 2019 flood over the Jamalpur district for event validation.

Meanwhile, the Haor basin of Northeast Bangladesh sees significant yearly flooding which often encompasses large uninterrupted swaths of inundation, in contrast to the more fragmented flood geography of the Brahmaputra regions.

While flash floods are common in this region, flooding can still wreak havoc on agriculture if

poorly timed, as happened in April 2017 when a flash flood came several weeks early and destroyed rice crops. This flood within the Sylhet District is also examined for validation purposes.

### III. Data and Methods

#### Data:

**Sentinel-1** is a constellation of two C-Band Synthetic Aperture Radar (SAR) imaging satellites launched in 2014 and 2016 by the European Space Agency (ESA). Radar backscatter data is available at 10m spatial resolution with revisit frequency of 6 days on average in Northern Bangladesh, often taking the form of a repeating 2-day and 10-day revisit cycle. Data in Northern Bangladesh scales up significantly in 2017 is therefore only usable 2017-Present (Fig 4.)

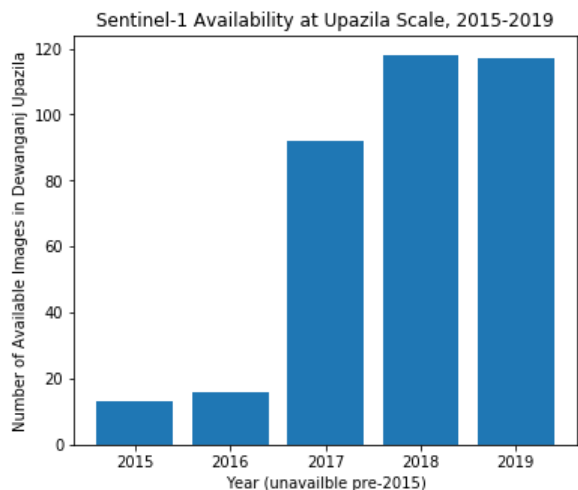


Figure 4: Bar graph showing the scale up of data availability with the Dewanganj Upazila in Jamalpur as a test case.

Data from Sentinel-1 is acquired and processed in Google Earth Engine (GEE). GEE hosts Sentinel-1 Ground Range Detected (GRD) scenes which are pre-processed through the Sentinel-1 Toolbox in order to 1. update the orbital metadata with a restituted orbit file, 2. remove artificially low values from image edges, 3. remove thermal noise, 4. calibrate to backscatter intensity in decibels (dB), and 5. terrain correct for high latitudes. From this image stack in GEE, the dual polarization of VV + VH bands in Interferometric Wide Swath (IW) were selected for study.

**SSM/I** is a Passive Microwave Radiometry (PMW) sensor which offers brightness temperature readings with twice daily coverage globally from 1979-Present. We take only ascending passes of Soil Moisture (providing daily data) at 3.125km resolution - gridded down from 25 km according to the rSIR antenna gain function (Brodzik et al., 2018).

Time series validation was conducted through comparisons to water danger levels. The Bahadurabhad river station on the Brahmaputra river in eastern Jamalpur was selected for a water level analysis because data was obtained through 2017 allowing comparison with both SSM/I and Setnienl-1, and a danger level of 19.5m is provided for this river station from the Bangladesh government.

For flood event validation, Sentinel-2 optical images are obtained for validation through GEE for flood events. Sentinel-2 images are available at 10m resolution for Red, Green, Blue, and NIR bands, and at 20m resolution for both SWIR bands. A water visualization of RGB = (SWIR2, SWIR1, Red) is used to highlight bodies of water. Clouds are masked from the Sentinel-2: Cloud Probability dataset with a <70% threshold used to mask the majority of clouds.

#### Algorithm:

##### **Sentinel-1:**

A Sentinel-1 time series is created by adapting a statistical deviation approach for flood mapping proposed by DeVries et al (2020). This algorithm selects a baseline of images over the study area from a dry historical period and compares flood images for statistical deviation.

##### **Sentinel-1 Algorithm Outline:**

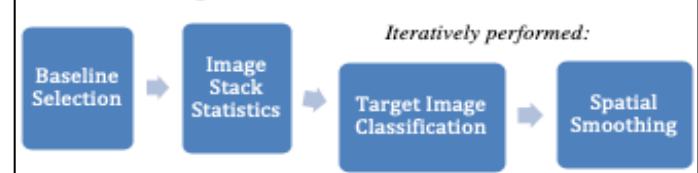


Figure 5: Algorithm outline of Sentinel-1 time series development

### Baseline Selection:

We adapt DeVries for application in Northern Bangladesh with a method for automatic baseline selection according to region. Due to rice irrigation schedules differing between districts, significant inundation may be present even in the traditional dry season, which in turn would systematically underpredict values for inundated area by decreasing statistical deviation between baseline and flood pixels. For example, districts among the District often sees significant inundation in January–February (Fig. 6) while the Sylhet Division might only reach the driest period in February–March.



Figure 6: Irrigated rice fields during Bangladesh dry season

To account for this regional variability in baseline periods, a “dry” 1.5 months for each district is derived as the period which gives the maximum 45 day moving average of a (Soil Moisture)<sup>-1</sup> time series between the general Bangladesh dry season period of November–March – demonstrated for Jamalpur District between 2017–2019 (Fig. 7). Soil Moisture is obtained by normalizing the surface soil moisture band of the NASA-USDA Global Soil Moisture Data in GEE.

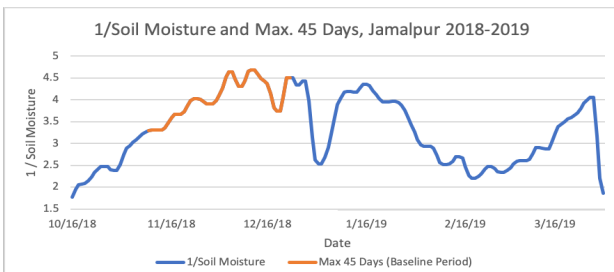


Figure 7: Illustration of Baseline selection in Jamalpur from inverse of normalized Soil Moisture plot.

### Image Stack Statistics:

From this baseline period of Sentinel-1 images, the image stack is split by orbital direction, and images with both VV and VH polarization are chosen. Mean backscatter, standard deviation, and backscatter anomaly is then calculated for each image in the two directional stacks. If a pixel is marked as water in >80% of the baseline images, that pixel is considered Permanent Open Water in all target images. If a pixel is marked as water in >25% of baseline images, the pixel is marked as having prior inundation for all images in the target stack.

A “target stack” is then created between the start and end date of study, and for each image in this target stack the z-score for each pixel is calculated from the baseline statistics.

### Target Image Classification:

Each image in the target stack is then iteratively classified by pixel. Pixels are ignored if previously marked as Permanent Open Water. Pixels are then defined as high confidence flood area if the pixel z-score for each polarization ( $Z_{VV}$ ,  $Z_{VH}$ ) is less than a z-score threshold for each polarization ( $thd_{VV}$ ,  $thd_{VH}$  = -2.5), with recommended threshold values derived from DeVries et al.

### Spatial Smoothing

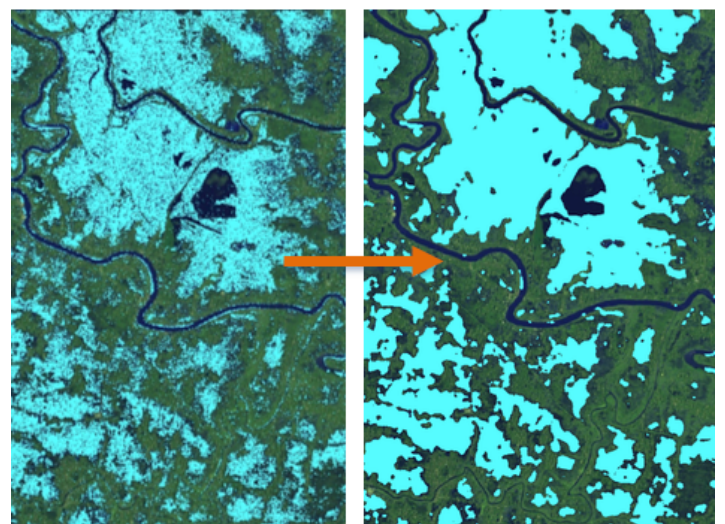


Figure 8: Smoothing algorithm demonstration. Right: raw algorithm, Left: smoothed with two kernels as described

In order to reduce radar noise typical of Synthetic Aperture Radar data, we implement a two-step spatial smoothing process demonstrated in Fig. 8. A pixel is marked as flooded if the focal mean of radius 4 is greater than 0.4 or the focal mean of radius 2 is greater than 0.5. After smoothing the image represents the final algorithm flood map. It is reduced on the district scale and divided by total district area in order to generate fractional flooded area.

**SSM/I:** In order to derive an inundation time series suitable for index insurance implementation, a variation of an algorithm for Passive Microwave flood detection proposed by DeGrove and Riva (2009) is performed over the brightness temperature time series. A “dry” calibration pixel is determined for each pixel from the 95<sup>th</sup> percentile of a 14x14 window centered at the pixel. For each date, a ratio of this calibration pixel (C) vs the pixel’s measured brightness temperature value (M) is calculated, denoted as the C/M ratio. When a pixel is flooded, the M decreases and C remains constant, leading to a peak in the C/M signal. From this signal, a flood magnitude metric is developed according to the form:

$$MA(t) = \frac{\frac{C}{M(t)} - \text{mean}(\frac{C}{M})}{\text{std}(\frac{C}{M})}$$

This magnitude value is thresholded at 2 standard deviations for each pixel to denote a flooded pixel, as proposed by DeGrove and Riva for regular flooding and verified as the most consistent flood signal by preliminary water level comparisons. From this algorithm results a daily inundation time series at 3.125km resolution from 1992-Present.

### Validation Approach:

To analyze and validate the behavior of each sensor’s time series, Brahmaputra water level and danger level data is qualitatively compared to the flooded area fraction time series from both Sentinel-1 and SSM/I. Expected behavior entails peaks in

fractional flooded area when water level exceeds danger level, a representation of the river overflowing and inundating nearby fields.

In order to validate the accuracy of each inundation time series over specific flood events, flood maps produced by both algorithms are compared to validation flood maps derived from optical Sentinel-2 images.

Two image validation approaches – spatial and random stratified sample – were used for this validation due to regional and data limitations. For the April 2017 flash flood in Sylhet, spatial validation was chosen due to the presence of clearly defined water and non-water bodies and cloud free Sentinel-2 images shortly after the Sentinel-1 image. A largely cloud free Sentinel-2 image (4/12/2017) is available 3 days after the chosen Sentinel-1 image (4/9/2017), however through analysis of the SSM/I time series and Landsat images from 4/8/2017, it was determined that flood extent remained largely constant in the ROI for this 3 day window. An SSM/I image was chosen from 4/9/2017 to ensure consistency with Sentinel-1.

For Sentinel-1, a 7.4 km<sup>2</sup> region of interest (ROI) was selected from the Sylhet District with both significant land and water coverage encompassing approximately 74,000 pixels. Due to a much larger SSM/I pixel size, a larger 242 km<sup>2</sup> region of interest encompassing the Sentinel-1 region was chosen for SSM/I validation encompassing 25 SSM/I pixels.

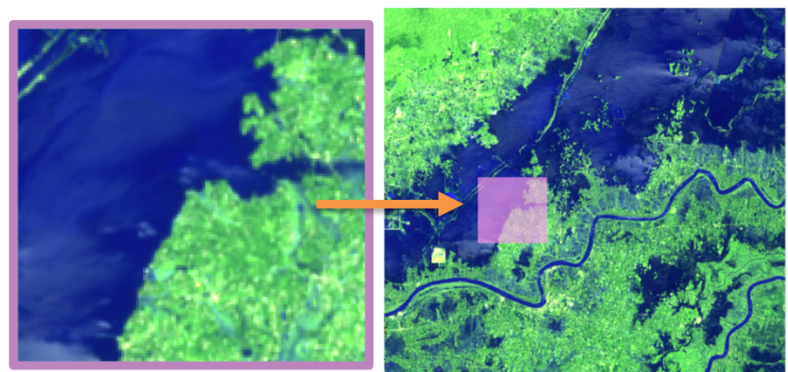


Figure 9: Sentinel-1 ROI (left) shown within SSM/I ROI (right)

For both ROIs, a Modified Normalized Difference Vegetation Index (MNDWI) image was

computed from the Sentinel-2 Image by the formula:

$$MNDWI = \frac{Green - SWIR2}{Green + SWIR2}$$

(Xu, 2017), and thresholded at 0.4, which proved to offer greatest accuracy requiring the least manual correction. The MNDWI images are then manually corrected in GEE to account for error in flooded area (Fig 10).



Figure 10: MNDWI demonstrated over Sentinel-1 ROI. Left: raw MNDWI image, Right: manually corrected MNDWI image

A final Baseline correction procedure is calculated for the Sentinel-1 ROI only, because the Sentinel-1 flood algorithm measures statistical deviation of the flood image to the baseline image and thus would not mark flooded pixels with prior inundation as flooded. The MNDWI process described for the flood image is repeated for a cloud free image in the dry baseline, and then subtracted from the flood MNDWI image in order to create an accurate image for new inundation (Fig. 11)

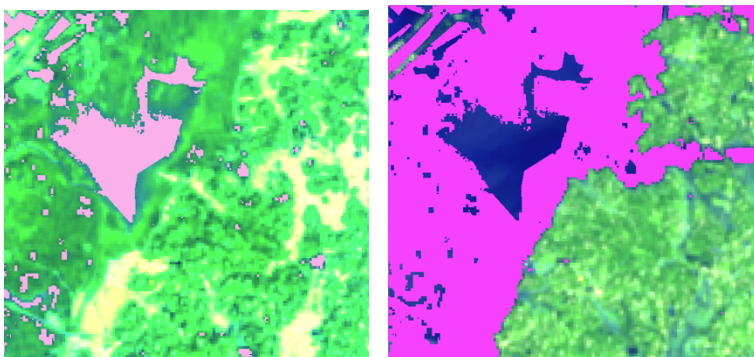


Figure 11: Baseline MNDWI image (left) and resulting new inundation image (right)

For validation of the July 2019 flood in Jamalpur, a random stratified sample approach was chosen due to a combination of scattered cloud

cover and high spatial variability between land and water - making a clear spatial classification difficult (Fig. 12).

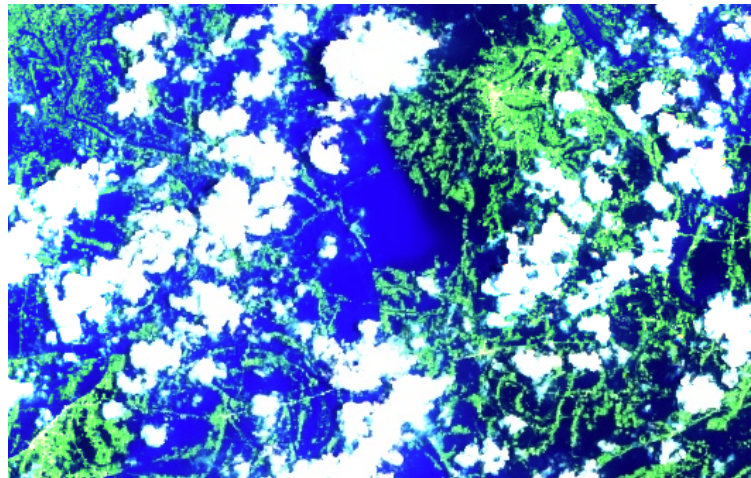


Figure 12: Typical cloud cover and land/water distribution in Jamalpur 2019 flood event making a spatial validation difficult.

From a cloud free Sentinel-2 image encompassing the entire district, points were chosen from three categories: land, flooded land, and permanent water (water in Sentinel-1 baseline and in flood image). A rough distribution for these points was estimated from an MNDWI calculation and found to be 140, 146, and 14, respectively.

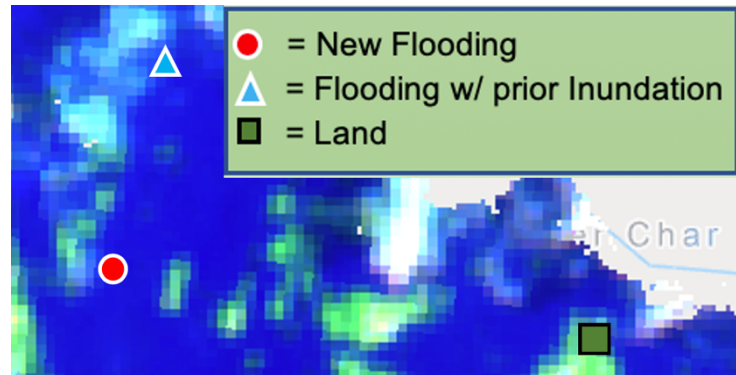


Figure 13: Example of 3 points representing the three classification values for sampled points

Each point was manually corrected to ensure accurate classification, and 39 points were removed due to cloud cover not algorithmically masked, cloud shadows, or an unclear division between land and water.

Metrics were calculated with “*flooding with prior inundation*” marked as *flooded* in the SSM/I analysis and *not flooded* for Sentinel-1 analysis, according to the algorithmic distinctions outlined in spatial validation.

The F1 metric for accuracy was chosen as a primary accuracy metric as it takes into account both false positives and false negatives. F1 was calculated by summing total true positive, false positive, and false negative Sentinel-2 pixels for each test and each sensor by the equation:

$$F1 = 2 * \frac{P*R}{P+R} = \frac{tp}{tp + \frac{1}{2}(fp+fn)},$$

where P = precision, R = recall, tp = true positive, fp = false positive, and fn = false negative. Additionally, bias is computed as:

$$Bias = \frac{A_r/A_v}{A_v/A_r}$$

where  $A_r$  represents total inundated area from the radar algorithm being tested and  $A_v$  represents inundated area in the validation image (Sampson et al, 2015). A bias of 0 to 1 represents underprediction and 1 to  $\infty$  represents overprediction of the radar algorithm.

## IV. Results

### Water Level Time Series:

Qualitative comparisons of SSM/I and Sentinel-1 to water level data suggests correlation between both sensors and water level behavior. While water level behavior is not expected to be directly correlated to fraction of district flooded, significant spikes in flooded area are expected when water level reaches above danger level, and the height of those water peaks above danger level can be expected to have some correlation with flood extent.

Fig. 14 shows that SSM/I displays peaks both times water level exceeds the danger level, and

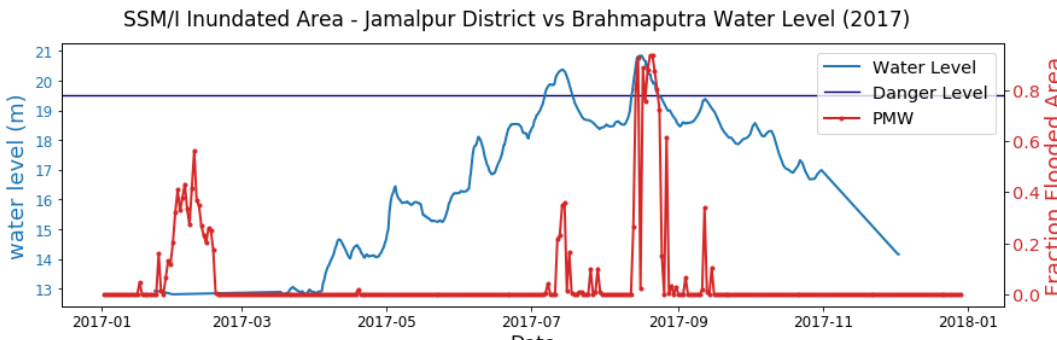


Figure 14: Water Level to SSM/I comparison

the second of these two peaks is larger than the first of these two peaks, expected by water level behavior. An inundation peak in January–February exist independent of any rise in water level, explained by aforementioned irrigation inundation occurring in areas near the Brahmaputra in January–February.

However, some inconsistency does exist in this SSM/I inundation time series. The time series dips to ~0 in August despite water level > danger level. Additionally, the peak value of fractional inundated area is ~1.0, representing the entire district as flooding. Flooding in Jamalpur takes the form of scattered bodies of water thus a value of 100% flooded area can be considered a significant overprediction in the SSM/I signal

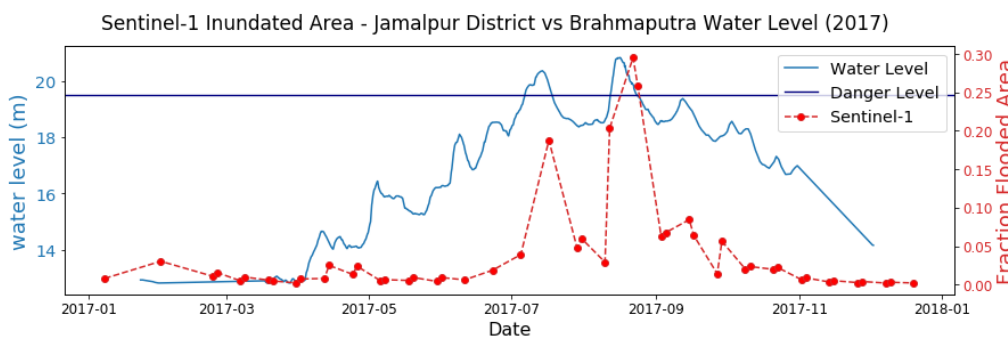


Figure 15: Water level to Sentinel-1 comparison

Fig. 15 similarly shows Sentinel-1 displaying behavior consistent with the water level time series. Two significant peaks are visible according to two peaks of water level, and inundated area for each is visibly related to the size of water level peaks.

Inconsistencies seen in the SSM/I signal are not present in the Sentinel-1 signal, and the early year irrigation spike is significantly less prominent. Furthermore, the Sentinel-1 signal displays systemically much lower values of inundation, with a maximum at ~30% inundation vs ~100% inundation in the SSM/I signal.

### Spatial Event Validation:

Spatial analysis of the Sentinel-1 and SSM/I flood maps over the April 2017 Haor Basin flood reveals higher accuracy and a superior bias metric in Sentinel-1 vs. SSM/I.

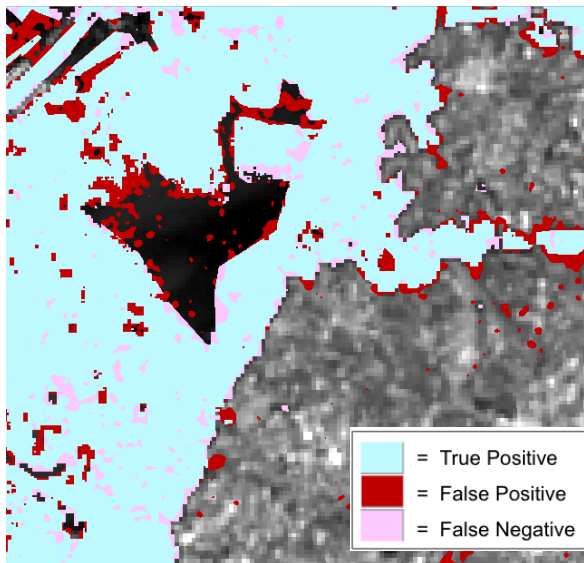


Figure 16: Sentinel-1 accuracy analysis over April 2017 Sylhet flash flood

The Sentinel-1 flood map (Fig. 16) shows mostly true positives over wide areas of inundated area, with false positives and false negatives largely occurring at borders of water and land or in areas where land and water is mixed.

However, qualitatively the algorithm largely distinguishes between water bodies and land at a small scale and accurately predicts inundation.

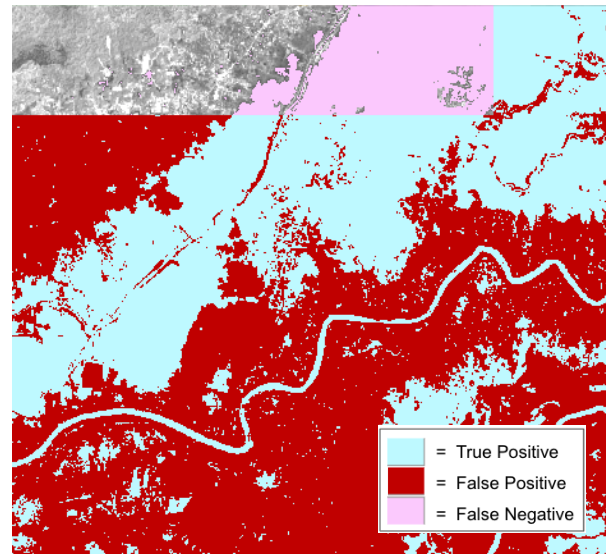


Figure 17: SSM/I accuracy analysis over April 2017 Sylhet flash flood.

Despite a significant expansion of the SSM/I ROI from the Sentinel-1 ROI to include 25 pixels over 242 km<sup>2</sup>, the SSM/I flood map (Fig. 17) still appears spatially inaccurate. Large sections of false positive readings even over significant stretches of land demonstrate the signal saturating around a flood event despite pixels having little inundation.

Accuracy Metrics for Event Validation				
	Sentinel-1		SSM/I	
	F1	Bias	F1	Bias
<b>Spatial Analysis (Sylhet, 2017)</b>	0.92	1.1	0.56	4.2
<b>Sampling Analysis (Jamalpur, 2019)</b>	0.84	0.85	0.67	4.7

Figure 18: Accuracy metrics (F1 and Bias) for Sentinel-1 and SSM/I over the two validation dates.

Fig. 18 provides accuracy metrics for both sensors over both spatial and random stratified sampling validation. We find significantly higher accuracy in Sentinel-1 than SSM/I, and bias in Sentinel-1 is relatively close to 1 while SSM/I overpredicts leading to biases of 4.2 and 4.7.

## Fusion Attempts:

Preliminary Sentinel-1 and SSM/I fusion tests were additionally performed similar to those proposed in Zeng, 2020. However, no significant correlation between an M/C ratio (inverse of aforementioned C/M ratio) and Sentinel-1 Flooded Area was discovered, and the quadratic fit described in Zeng, 2020 only resulted in a fit of  $R^2 = 0.072$  (Fig 19).

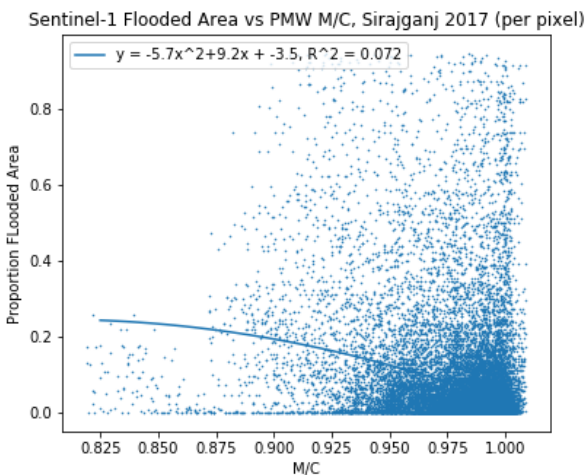


Figure 19: preliminary fusion attempt at per pixel M/C to fraction flooded area comparison.

Higher correlations were found when pixels were examined individually, however fit characteristics and correlation varied widely between pixels.

## V. Discussion and Recommendation

Overall, Sentinel-1 demonstrates a far higher ability to accurately detect floods and develop an inundation time series in Northern Bangladesh. Sentinel-1 demonstrates higher accuracy and a bias closer to 1 in event validation, and in time series comparisons to water level shows a clearer relationship with water level and danger level.

However, Sentinel-1 does appear to underpredict inundation extent and be less accurate in regions with more scattered and varied flood geography such as in Jamalpur, as qualitatively observed in flood maps and demonstrated numerically through a lower bias in Jamalpur vs Sylhet validation.

Additionally, significant flaws exist with the availability of Sentinel-1 data. A repeat cycle which is 6-days on average yet in Northern Bangladesh often takes the form of 2- and 10-day repeating cycles could lead to a major yet short flood event being altogether missed by the algorithm or underpredicted. Despite water level data not showing any large flood events missed by Sentinel-1, a larger scale study is needed to determine the likelihood of Sentinel-1 significantly underpredicting or missing a large flood event.

Furthermore, as data for Sentinel-1 is only practically available (>30 observations a year) from 2017-Present, there is no way to quantify flood risks over a long time period as is necessary for an index insurance application.

Despite these challenges, Sentinel-1 still offers an exciting and proven alternative to optical sensors for flood mapping in Bangladesh and for index insurance implementations. The Sentinel-1 time series is demonstrated to be consistent, spatially accurate, and available in all conditions and weather.

In contrast, SSM/I faces larger challenges in acting as a reliable indicator of inundation over time. Despite a time series which aligned to water level temporally, concerns about significant spatial inaccuracies make its use for index insurance difficult without greater development.

However, due to its advantages in availability – several decades of data with twice daily passes – the SSM/I Passive Microwave Sensor still holds great promise for gathering temporal and historical information about flood events in Bangladesh. With a more complex flood algorithm and temporal smoothing processes which increase accuracy, the SSM/I signal could serve as a reliable indicator for when flood events begin, how often they have and will occur, and how their behavior varies over different years.

The possibility of sensor fusion holds promise despite poor results described above. Future work could include a per-pixel fit approach to Synthetic Aperture Radar and Passive Microwave flood fusion in order to increase temporal accuracy of the Sentinel-1 flood signal.

SSM/I will always be bounded by spatial resolution constraints, but through a combination of Sentinel-1 for spatial flood information and SSM/I for historical risk assessment and fine temporal behavior, multiple radar technologies could effectively combine for flood index insurance in Bangladesh.

Further, even without supplementation from SSM/I, Sentinel-1 demonstrates ability to function as an index insurance trigger for future flood events and develop a reliable, consistent, and accurate inundation time series in Northern Bangladesh.

### Current Applications:

Sentinel-1 data as an indicator of flooding in Northern Bangladesh has current applications including and beyond index insurance. Recent July 2020 floods in Bangladesh present an opportunity to implement the Sentinel-1 algorithm for disaster relief and to validate information on the ground.

Flood maps were made for this flood both for July 20-21 and July 26-27 (two dates near the flood peak) and sent to Green Delta, an insurance company piloting flood index insurance with MODIS. These maps (ex. Fig. 21) give valuable validation data for current implementations, can

help guide policy and relief (Fig. 20), and serve as a proof of concept for future use as an index insurance trigger.

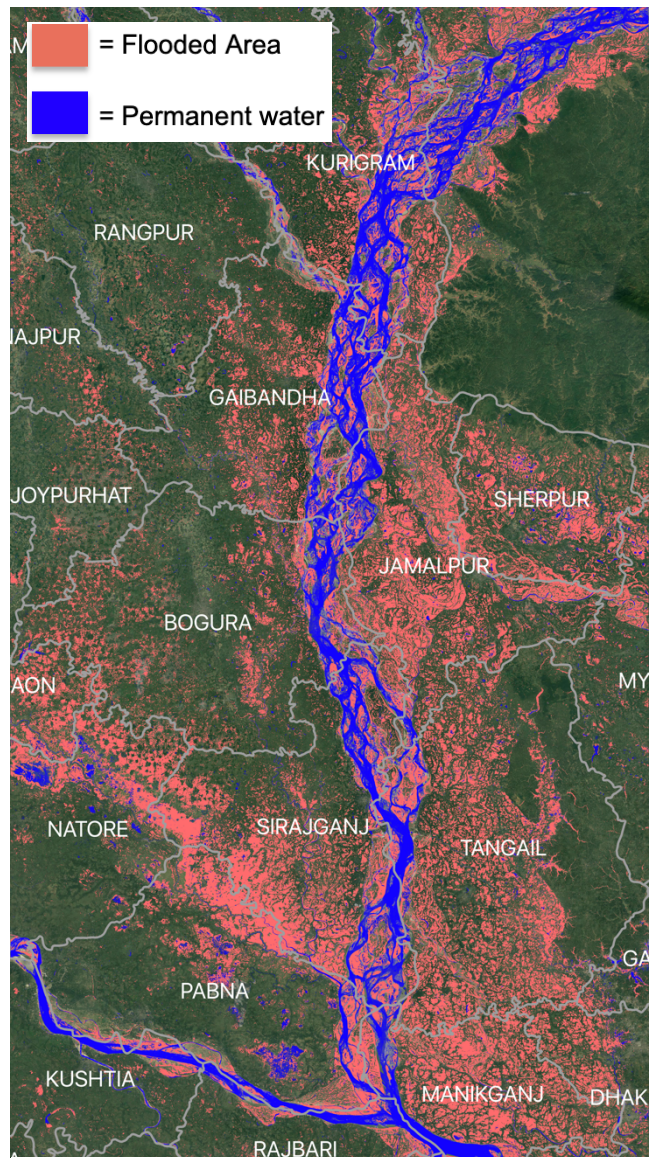


Figure 21: 7/27 inundation map over Brahmaputra region

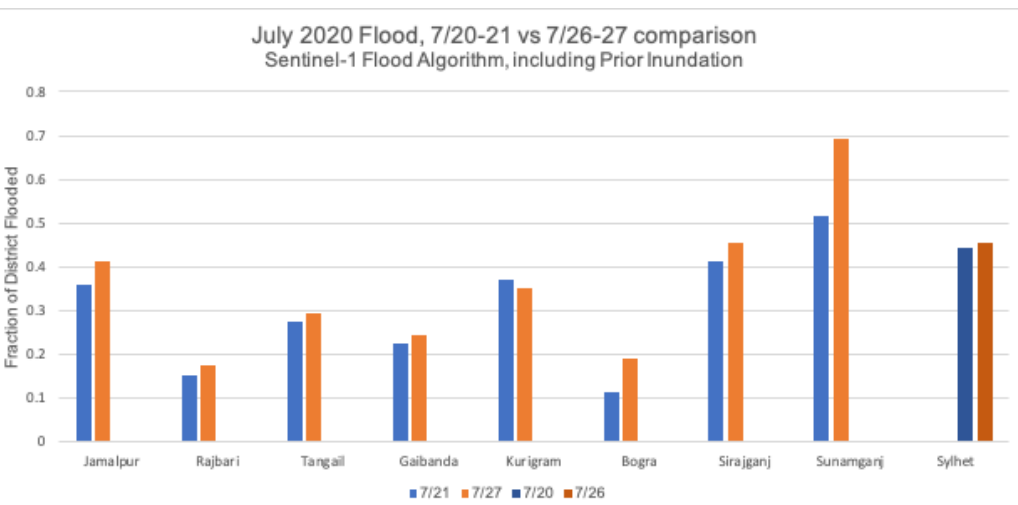


Figure 20: District-level comparison between 7/20-7/21 inundation and 7/26-7/27 inundation

## **Reference:**

- Amarnath, G. (2020). *First satellite-based insurance trial in Bangladesh helps farmers recover from flooding CCAFS: CGIAR research program on Climate Change, Agriculture and Food Security*. CCAFS. <https://ccafs.cgiar.org/research-highlight/first-satellite-based-insurance-trial-bangladesh-helps-farmers-recover-flooding#.XzalGRNKhhE>
- Brodzik, M. J., Long, D. G., Hardman, M. A., Paget, A., & Armstrong, R. L.: MEaSURES Calibrated Enhanced-Resolution Passive Microwave Daily EASE-Grid 2.0 Brightness Temperature ESDR, Version 1; National Snow and Ice Data Center: Boulder, CO, USA, Digital Media, doi: <https://doi.org/10.5067/MEASURES/CRYOSPHERE/nsidc-0630.001>, 2016. Updated 2018.
- Davies, R. (2017, April 7). *Bangladesh – Floods in North East Wipe Out Rice Crops – FloodList*. FloodList. <http://floodlist.com/asia/bangladesh-floods-north-east-wipe-rice-crops>
- De Groot, T., & Riva, P. (2009). Global real-time detection of major floods using passive microwave remote sensing. *Proceedings, 33rd International Symposium on Remote Sensing of Environment, ISRSE 2009*, 587–590.
- DeVries, B., Huang, C., Armston, J., Huang, W., Jones, J. W., & Lang, M. W. (2020). Rapid and robust monitoring of flood events using Sentinel-1 and Landsat data on the Google Earth Engine. *Remote Sensing of Environment*, 240, 111664. <https://doi.org/10.1016/j.rse.2020.111664>
- Landuyt, L., Van Wesemael, A., Schumann, G. J. P., Hostache, R., Verhoest, N. E. C., & Van Coillie, F. M. B. (2019). Flood Mapping Based on Synthetic Aperture Radar: An Assessment of Established Approaches. *IEEE Transactions on Geoscience and Remote Sensing*, 57(2), 722–739. <https://doi.org/10.1109/TGRS.2018.2860054>
- Xu, H. (2006). Modification of normalised difference water index (NDWI) to enhance open water features in remotely sensed imagery. *International Journal of Remote Sensing*, 27(14), 3025–3033. <https://doi.org/10.1080/01431160600589179>
- Zeng, Z., Gan, Y., Kettner, A. J., Yang, Q., Zeng, C., Brakenridge, G. R., & Hong, Y. (2020). Towards high resolution flood monitoring: An integrated methodology using passive microwave brightness temperatures and Sentinel synthetic aperture radar imagery. *Journal of Hydrology*, 582, 124377. <https://doi.org/10.1016/j.jhydrol.2019.124377>